

## Multi-point monitoring of cross-linking reactions

Machavaram, Venkata Rajanikanth; Wang, Liwei; Pandita, Surya Darma; Hellmann, Sebastian; Bogonez, Francisco Nieves; Fernando, Gerard Franklyn

DOI:

[10.1002/app.41088](https://doi.org/10.1002/app.41088)

License:

Creative Commons: Attribution (CC BY)

*Document Version*

Publisher's PDF, also known as Version of record

*Citation for published version (Harvard):*

Machavaram, VR, Wang, L, Pandita, SD, Hellmann, S, Bogonez, FN & Fernando, GF 2014, 'Multi-point monitoring of cross-linking reactions', *Journal of Applied Polymer Science*, vol. 131, no. 22, 41088.  
<https://doi.org/10.1002/app.41088>

[Link to publication on Research at Birmingham portal](#)

### **Publisher Rights Statement:**

Eligibility for repository : checked 1/08/2014

### **General rights**

Unless a licence is specified above, all rights (including copyright and moral rights) in this document are retained by the authors and/or the copyright holders. The express permission of the copyright holder must be obtained for any use of this material other than for purposes permitted by law.

- Users may freely distribute the URL that is used to identify this publication.
- Users may download and/or print one copy of the publication from the University of Birmingham research portal for the purpose of private study or non-commercial research.
- User may use extracts from the document in line with the concept of 'fair dealing' under the Copyright, Designs and Patents Act 1988 (?)
- Users may not further distribute the material nor use it for the purposes of commercial gain.

Where a licence is displayed above, please note the terms and conditions of the licence govern your use of this document.

When citing, please reference the published version.

### **Take down policy**

While the University of Birmingham exercises care and attention in making items available there are rare occasions when an item has been uploaded in error or has been deemed to be commercially or otherwise sensitive.

If you believe that this is the case for this document, please contact [UBIRA@lists.bham.ac.uk](mailto:UBIRA@lists.bham.ac.uk) providing details and we will remove access to the work immediately and investigate.

## Multi-Point Monitoring of Cross-Linking Reactions

Venkata Rajanikanth Machavaram,<sup>\*</sup> Liwei Wang,<sup>†</sup> Surya Darma Pandita, Sebastian Hellmann, Francisco Nieves Bogonez, Gerard Franklyn Fernando

School of Metallurgy and Materials, University of Birmingham, Edgbaston, Birmingham B15 2TT, United Kingdom.

<sup>\*</sup>Present address: School of Electronics Engineering VIT University, Vellore-632 014 Tamil Nadu, India.

<sup>†</sup>Present address: Department of Chemistry and Chemical Engineering, Minjiang University, Fuzhou 350108, People's Republic of China.

Correspondence to: G. F. Fernando (E-mail: g.fernando@bham.ac.uk).

**ABSTRACT:** The feasibility of deploying optical fiber sensors to obtain qualitative and quantitative information on the cross-linking characteristics of thermosetting resin systems has been demonstrated by a number of researchers. This article is concerned with the demonstration of a low-cost fiber-optic Fresnel sensor system for monitoring the cross-linking reactions at multiple locations. Cross-linking reactions can be influenced by a number of parameters including the stoichiometry of the resin and hardener, and the heat-transfer rates in and out of the preform as a function of the cross-section of the preform. In situations where there is a variation in the thickness of the preform or when large components are processed, a facility to monitor the cross-linking reactions at multiple locations will be valuable because the rate and extent of the cross-linking can be inferred. In this article, six Fresnel sensors were immersed in individual vials containing an epoxy/amine resin system and processed (cross-linked) in an air-circulating oven. One additional vial with a Fresnel sensor immersed in the neat epoxy resin (no hardener) was co-located in the oven to enable the effect of temperature to be monitored. The feasibility of using the multiplexed Fresnel sensors for cure monitoring was demonstrated successfully. The sensors in the post-cross-linked samples were used to study the effects of heating and cooling cycles. The feasibility of detecting the glass transition temperature using the Fresnel sensor is discussed along with the factors that give rise to variability in the output Fresnel signals. © 2014 The Authors. Journal of Applied Polymer Science Published by Wiley Periodicals, Inc. *J. Appl. Polym. Sci.* **2014**, *131*, 41088.

**KEYWORDS:** cross-linking; resins; manufacturing; optical properties; thermosets

Received 5 December 2013; accepted 27 May 2014

**DOI:** 10.1002/app.41088

### INTRODUCTION

Thermosetting resins are used extensively as adhesives, coatings, and matrices for fiber reinforced composites. In general, thermosets consist of two primary components namely; the resin and hardener.<sup>1</sup> In a typical manufacturing operation, the resin and hardener are weighed in the required stoichiometric ratio and mixed thoroughly prior to use. Depending on the chemical reactivity of the hardener, the cross-linking reaction can be initiated at room-temperature or by the application of heat. The transformation of the mixed resin and hardener from a liquid (or semi-solid) state to a highly cross-linked structure is commonly referred to as “curing”.

Generalized cross-linking reaction schemes between an epoxy resin and an amine hardener are illustrated in Figures 1(a,b).<sup>1</sup> Figure 1(a) illustrates the reaction between an epoxy and amine

functional group that leads to the formation of a covalent bond between the two reagents, along with the formation of a hydroxyl group. In addition, it is seen that the primary amine is converted to a secondary amine. The secondary amine in turn can react with another epoxy group with the formation of a tertiary amine and another hydroxyl group; this is illustrated in Figure 1(b).

With reference to cross-linking of thermosets illustrated in Figures 1(a, b), the following additional comments can be made.

- i. The resin and the hardener are generally mixed manually prior to initiating the cross-linking reaction via the application of heat. The issue here is the homogeneity of the mixed resin system and the possibility of entrapped and dissolved gasses. Hence, it is a common practice to de-gas the mixed resin in a vacuum chamber prior to use. A facility to track the progression of the cross-linking reaction in

This is an open access article under the terms of the Creative Commons Attribution License, which permits use, distribution and reproduction in any medium, provided the original work is properly cited.

© 2014 The Authors. Journal of Applied Polymer Science Published by Wiley Periodicals, Inc.

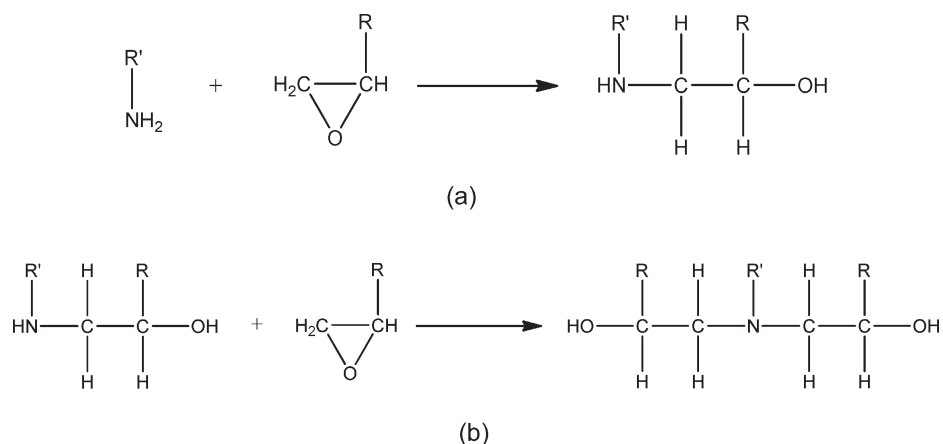


**Figure 1.** General reaction schemes for epoxy and amine-based reactions: (a) primary amine-epoxy addition; and (b) secondary amine-epoxy addition.

real-time, against a previously determined profiles, will offer a means for appropriate remedial action to be taken in the event that a deviation is observed.

- ii. The molecular weight of the resin system increases over the course of the reaction in proportion to the cross-link density. As a consequence, the density of the resin system and the refractive index increase during the cross-linking reactions. Therefore, there is significant interest in developing techniques to monitor the evolution of the molecular weight and the refractive index in real-time.
- iii. The ring-opening reactions are exothermic. Therefore, the volume of the resin system used can have a major bearing on the temperature attained within the reaction vessel; in other words, the actual peak temperature experienced by the resin can be significantly higher than the set or desired isothermal condition. Hence, efficient thermal management and accurate monitoring of the temperature is important if data on the cross-linking kinetics are required.
- iv. In a typical cure schedule, the resin system is heated from ambient to the desired isothermal value and it is held at this point for a specified time (dwell). The viscosity of the resin system initially reduces as the temperature is increased from ambient to the desired isothermal temperature. At some stage during the temperature-ramp, the resin system starts to cross-link and consequently, the viscosity and the refractive index increase rapidly. This increase in the viscosity reaches a point where the liquid resin system is converted to a gel; this is generally referred to as the gel-point. The other important stage in the processing of thermosets is vitrification; this is the conversion of the gel to a glassy solid. Tools to identify these transitions in the resin system during processing will enable process optimization routines to be specified.
- v. The formation of covalent bonds between the resin and hardener leads to shrinkage in typical high-performance thermosetting resins. The shrinkage stresses can be high enough to cause debonding from the reinforcement or the container/substrate. There is significant interest developing technique to quantify the magnitude of the shrinkage associated with thermosetting resin systems.
- vi. During the heating phase of the mixed resin system and the reinforcement, the constitutive components expand. It

is important to appreciate that the peak temperature experienced will be a function of the set isothermal value, the thermal management and the magnitude of the exotherm. At some stage in the cross-linking process, “bonding” between the surface of the fiber reinforcement and the matrix will occur and this may be a combination of chemically and/or mechanically induced processes. Cooling the material from the processing temperature to ambient will result in the generation of residual fabrication stresses. Residual stresses can initiate debonding and cracking in composites materials even without the application of mechanical load. Furthermore, they can also lead to warping and loss of dimensional stability.

- vii. The glass transition temperature of the cross-linked resin system represents a second-order thermodynamic transition where the properties such as the heat capacity, thermal expansion, and the stiffness undergo reversible changes over a specified temperature range. Therefore, there is significant merit in developing techniques to monitor the occurrence of the glass transition temperature.

With reference to the above-mentioned issues, the ability to monitor progression of the cross-linking reaction at multiple points in the preform may be necessary in some instances. For example, in situations where the cross-section of the preform changes or when thick laminated preforms are being processed. A number of the above-mentioned topics and parameters can be accessed and/or monitored using optical fiber-based sensor systems.<sup>1</sup>

For example, extrinsic<sup>2</sup> and intrinsic<sup>3</sup> fiber Fabry-Perot interferometric sensors have been used for *in situ* strain monitoring. The extrinsic fiber Fabry-Perot interferometric sensor has also been adapted for monitoring temperature.<sup>4,5</sup> Intensity-based optical fiber sensors have been used for logging strain.<sup>6</sup> Fiber Bragg gratings continue to be used extensively for monitoring strain and temperature during the processing of fiber reinforced composites.<sup>7,8</sup> The feasibility of using combined strain and temperature monitoring via optical fibers has also been demonstrated.<sup>9</sup> Long-period gratings have been used for cure monitoring.<sup>10</sup> More recently, the feasibility of monitoring multiple parameters (strain, temperature, refractive index, and cross-

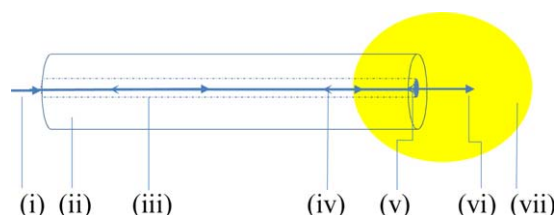


**Figure 2.** Schematic illustration of the Fresnel reflection at the cleaved-end of an optical fiber that is surrounded by the resin system. (i) Input light. (ii) Cladding. (iii) Core. (iv) Reflected light. (v) Fresnel reflection at the core/resin interface. (vi) Transmitted light. (vii) Resin system. [Color figure can be viewed in the online issue, which is available at [wileyonlinelibrary.com](http://wileyonlinelibrary.com).]

linking) using a single sensor and interrogation system was demonstrated.<sup>11</sup> Sensor designs for the quantitative monitoring of the relative concentrations of specified functional groups are predominantly based on transmission and reflection and evanescent wave near-infrared spectroscopy.<sup>12,13</sup>

As this article is concerned with Fresnel sensors, the following section provides a brief review of this intensity-based sensor design.

### Fresnel Reflection Sensors

Fresnel sensors are essentially based on the measurement of light reflected at the interface of two dielectric media owing to the discontinuity in the refractive index. A schematic illustration of the Fresnel reflection sensor is presented in Figure 2 where the cleaved fiber-end is shown to be surrounded in the resin system. The reflection at normal incidence is also indicated.

Light undergoing Fresnel reflection is governed by the refractive index contrast between the core of the optical fiber and the medium surrounding the cleaved-end. When light illuminates the interface of two dielectric media of refractive indices  $n_1$  and  $n_2$  at an angle of incidence of  $\theta_1$ , the coefficients of the reflected field amplitudes parallel ( $r_{||}$ ) and perpendicular ( $r_{\perp}$ ) to the plane of incidence can be expressed using the Fresnel equations<sup>14</sup>:

$$r_{\perp} = \frac{n_1 \cos \theta_1 - n_2 \cos \theta_2}{n_1 \cos \theta_1 + n_2 \cos \theta_2}; r_{||} = \frac{n_2 \cos \theta_1 - n_1 \cos \theta_2}{n_2 \cos \theta_1 + n_1 \cos \theta_2} \quad (1)$$

where  $\theta_2$  is the angle of refraction into the second medium. During normal incidence ( $\theta_1 = \theta_2 = 0$ ), the magnitudes of the field amplitudes are retained and the reflectivity “ $R$ ” at the interface can be expressed as:

$$R = \left( \frac{n_1 - n_2}{n_1 + n_2} \right)^2 \quad (2)$$

Optical fiber-based Fresnel reflection sensors have been used to track the changes in the refractive index of thermosetting resin systems during cross-linking.<sup>15–18</sup> For example, Crosby et al. reported on an optical fiber-based refractometer for monitoring the cross-linking of an epoxy/amine resin system.<sup>19</sup> The reflection from the cleaved-end of the fiber was calibrated using reference refractive index liquids. The response of the Fresnel reflection sensor showed a good correlation with the quantitative cross-linking kinetic data obtained using a conventional Fourier transform near-infrared spectrometer. Liu et al. reported

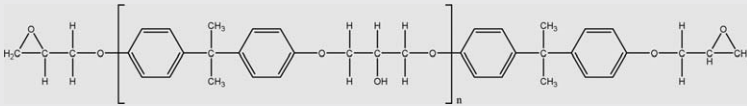
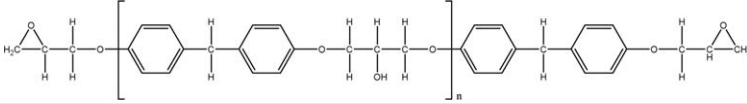
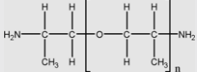
on a multipoint cure monitoring system that employed Fresnel reflection sensors in conjunction with optical time domain reflectometry.<sup>20</sup> The degree of conversions calculated from the calibrated Fresnel sensors were found to be in good agreement with data obtained from a differential scanning calorimeter (DSC). Huang et al. demonstrated a parallel multipoint Fresnel-based temperature sensor.<sup>21</sup> Chen et al. used the same sensor design concept to monitor the temperature and liquid concentration.<sup>22,23</sup>

Cusano et al. demonstrated a Fresnel reflection sensor using a modulated light source and a lock-in amplifier.<sup>24</sup> The degree of conversion obtained via the sensor was said to correlate with the DSC data.

It is generally accepted that intensity-based sensing techniques can suffer from fluctuations in the light source. This issue was addressed by Chang et al.<sup>25</sup> and Kim and Su.<sup>26</sup> They used a  $2 \times 2$  fiber coupler with a splitting ratio of 50 : 50, where one of the output arms (one of the cleaved fiber-ends) served as the sensing element and the other was spliced to a fiber spool and this cleaved-end served as a reference element. A pulse generator was used to modulate the laser source. The sensing arm of the coupler was placed in the liquid of interest whilst the other longer section of the reference arm was left in air. The reflected light from the cleaved fiber-ends were detected by a de-coupled detector. As the light source was modulated and because the lengths of the sensing and reference arms of the coupler were significantly different, it was possible for the two signals to be separated temporally. The dual-coupler-based sensor interrogation design of Buggy et al. enabled monitoring of the refractive index during the cure reaction of epoxy resin via UV-light irradiation.<sup>27</sup> The reflection from air served as the reference. Giordano et al. demonstrated an optical fiber sensing system for the simultaneous measurement of refractive index via Fresnel reflection, and strain via a fiber Bragg grating.<sup>28</sup> More recently, Mahendran et al. demonstrated a multifunctional sensor system where a conventional fiber-coupled FTIR near-infrared spectrometer was used to monitor four independent parameters simultaneously: strain, temperature, refractive index, and cross-linking kinetics of an epoxy/amine resin system.<sup>29</sup> Fiber-optic Fresnel sensors have also been used for cure monitoring of thermoset resins containing fillers<sup>30</sup> and during resin infusion.<sup>31</sup>

With reference to the routine manufacture of fiber reinforced composites in industry, in general, the same resin system is used over long periods for a given product range. This may be because of end-user specifications or to comply with certification requirements. In such circumstances, once the resin system has been characterized thoroughly in terms of its mechanical, thermal, optical, and chemical properties, on-line quality assessment can be provided by intensity-based sensor systems. Multi-point monitoring during processing can provide valuable information on the relative rates of reactions at specified locations within large preform or where there is a change in the cross-section. The advantage of intensity-based sensors is that they offer a low-cost option to infer the relative rates of reactions of thermosetting resin systems. As the sensors are embedded in the composites, they can be used in-service to monitor

**Table I.** Chemical Structure of the LY3505 Resin and XB3403 Hardener

Name	
LY3505 Bisphenol-A	
Bisphenol-F	
XB3403	

parameters that influence the refractive index of the cross-linked resin. For example, temperature and ingress and egress of fluids. The majority of the previous publications on the use of the Fresnel reflection sensor have been associated with primarily single sensors. With reference to the limited previous publications on multiplexed Fresnel reflection sensor designs, the device reported in the current publication is significantly simpler because it merely involves cleaved optical fibers. The rationale for the current work was to study the cross-linking behavior of a thermosetting resin system using a low-cost multiplexed Fresnel reflection sensor system. The evolution of the refractive index and the output from multiple Fresnel reflection sensors during the processing of an epoxy/amine resin system was monitored and analyzed in detail.

## EXPERIMENTAL

### Fresnel Sensor

The Fresnel sensors were manufactured from single-mode SMF-28 (Corning) fiber. These sensors were prepared by stripping the polymer buffer (protective coating) and cleaving the fibers using a conventional optical fiber cleaver. The cleaved-ends were cleaned with a lint-free tissue soaked in isopropanol and then dried and examined under a microscope to verify that the cleaved-end was perpendicular.

### Resin System

The epoxy resin system used was Araldite LY3505/XB3403 (Huntsman Advanced Materials, UK). The chemical structures of the two components, LY3505 and XB3403, are illustrated in Table I. These materials were used as-supplied without further purification. The resin and hardener were weighed out in the stoichiometric ratio of 100 : 35 (wt %) respectively. The two components were mixed manually and degassed in a vacuum chamber for 15 minutes. Approximately 2 mL of the degassed resin system was dispensed into individual glass vials of dimensions 12 mm (diameter), 50 mm (length), and a wall-thickness of 1.3 mm.

### Sensor Interrogation System

A schematic illustration of the experimental setup for the Fresnel sensor system is presented in Figure 3. An air-circulating oven was used to cross-link the resin system at specified temperatures. The cleaved optical fibers were secured rigidly inside

the glass vials, ensuring that they were positioned away from the bottom and the side walls. Approximately 2 mL of the premixed and degassed resin system was dispensed into six glass vials ensuring that the cleaved fiber-ends were immersed in the liquid; the immersion depth for the six Fresnel sensors was similar. A K-type thermocouple was also used in each vial to measure the temperature.

In addition to the above-mentioned glass vials, a Fresnel reflection sensor and a thermocouple were immersed in a vial containing the neat epoxy resin (without the hardener) and placed in the oven. A further glass vial containing index matching gel, a Fresnel sensor, and a thermocouple was placed outside the oven under ambient conditions.

With reference to Figure 3, the distal end of the Fresnel sensors were coupled to an automatic optical channel selector (MN9674A, Anritsu, UK) where each channel was scanned with a specified time interval. The channel selector was triggered externally via a data acquisition LabVIEW programme to obtain the reflected light signals from the Fresnel sensors in a sequential fashion. Light from a temperature-controlled laser diode with a wavelength centered at 1550 nm was coupled into the sensing fibers using a 50 : 50 coupler. The laser diode was mounted on a temperature-controlled laser diode mount (LDM-4984, ILX lightwave, USA) in conjunction with a modular laser diode controller (LDC 3900, ILX lightwave, USA). The reflected light signals from the Fresnel sensors were detected using an InGaAs photodiode detector (Thorlabs, UK) and a photodiode amplifier (PDA 200) in tandem with a low-noise preamplifier (Model SR560, Stanford Research Systems, USA). The data acquisition system was used to record the data from the Fresnel sensors and thermocouples.

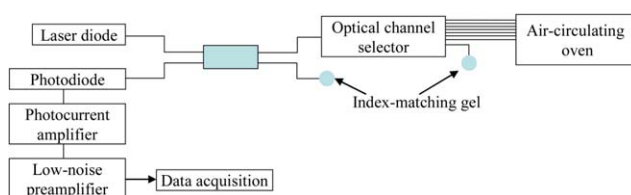


**Figure 3.** Schematic illustration of the experimental set-up for interrogating the multiplexed Fresnel reflection sensor system. [Color figure can be viewed in the online issue, which is available at [wileyonlinelibrary.com](http://wileyonlinelibrary.com).]



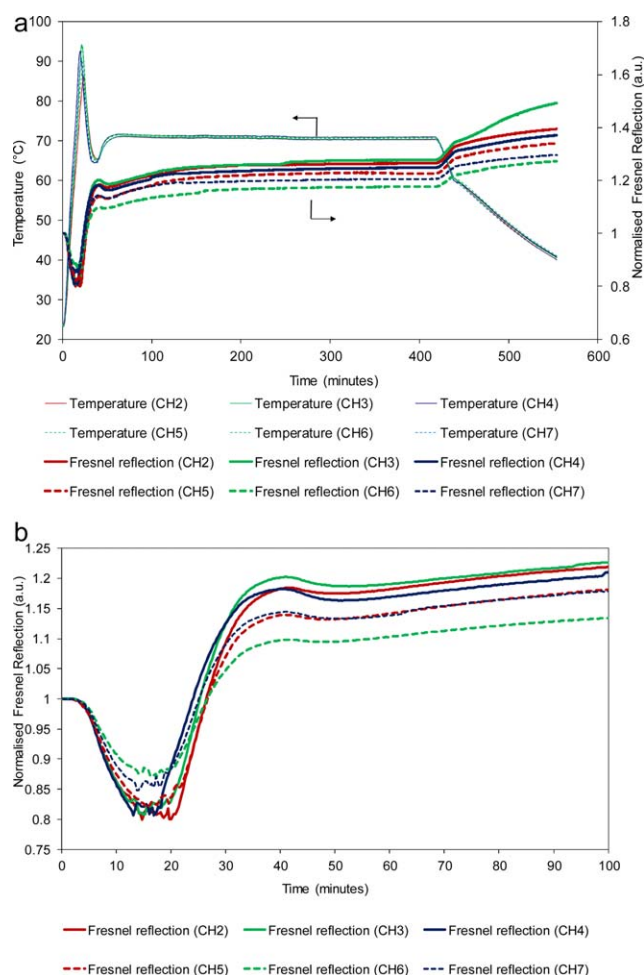


**Figure 4.** (a) Response of the six independent Fresnel reflection sensors and the corresponding temperature data from the thermocouples during cross-linking and cooling of the resin system in the oven. (b) Expanded view of Figure 4(a). [Color figure can be viewed in the online issue, which is available at [wileyonlinelibrary.com](http://wileyonlinelibrary.com).]

## RESULTS AND DISCUSSION

### Fresnel Reflection Sensor

The responses of the six individual Fresnel reflection sensors in the glass vials and the corresponding temperature data from the thermocouples during cross-linking in the oven are presented in Figures 4(a,b).

With reference to Figures 4(a), the cross-linking process was monitored through channels 2–7 of the optical channel selector. Channel 1 was used to monitor a Fresnel sensor that was immersed in index-matching gel but located outside the oven under ambient conditions. Channel 8 was used to monitor the Fresnel signal emanating from a cleaved optical fiber that was immersed in neat epoxy resin (no hardener), and located in the oven along with the other vials containing the mixed epoxy/amine resin. The response of each of the Fresnel sensors was normalized to its respective signal when the temperature of the oven was between 23°C and 24°C.

The outputs from each of the Fresnel sensors and the corresponding temperature of the resin system in the vials were

recorded simultaneously. The sequential switching of the array of Fresnel sensors via the optical switching unit was carried out automatically at an interval of 16 seconds.

The following section presents a discussion on the general trends observed in Figures 4(a,b).

- i. **Magnitude of the exotherm:** The magnitude of the exotherm recorded by the thermocouples is around 85–95°C; the set (desired) dwell temperature was 70°C. There are three possible reasons for this. Firstly, as the experiments were carried out in an air-circulating oven, it was not possible to compensate for the exotherm by cooling the container to maintain isothermal conditions. Secondly, the glass vials were placed on a PTFE block with holes drilled to accommodate the samples. Hence, the heat dissipation, originating from the exothermic cross-linking reactions, was not ideal. Finally, the magnitude of the exotherm is proportional to the volume of the resin used. In the current series of experiments, approximately 2 mL of the mixed resin system was dispensed manually via a syringe. However, the actual volume of the resin dispensed per vial may have varied slightly. The magnitude and the duration of the exotherm are important because it can influence the rate and the extent of the cross-linking reactions, and hence, the resultant properties of the thermosetting resin [32].
- ii. **Magnitude of the Fresnel signal:** The general trends in the outputs from the Fresnel sensors deployed in different vials containing resin system are similar. However, the magnitude of the reflected Fresnel signal is slightly different and this may be because of one or more of the following reasons: (a) approximately 5 m of fiber was used per sensor (distance between the glass vial containing the resin in the oven and the interrogation unit). Bend-induced losses along the fiber path and losses at the fusion splices may account in part to the observed small differences in the magnitude of the Fresnel signals; (b) the optical losses across the channels in the switching unit were quantified and the variation was found to be in the range of 2–10%; (c) the quality of the cleaved optical fiber is unlikely to be a contributing factor because each sensor was inspected prior to use. However, the possibility of localized variations in the homogeneity of the resin system, in the vicinity of the core of the cleaved optical fiber (9  $\mu\text{m}$ ), cannot be ruled out. The channel selector used in this work has a switching reproducibility of 0.02 dB or less at a constant temperature (manufacturer's data) within the operable temperature range of 0–50°C. The variation in the temperature in the laboratory, over the duration of the cross-linking experiments (12 hours), was 20–24°C. The variation in the output signal from channel 1 (Fresnel sensor immersed in the index matching gel but located outside the oven) over the duration of the experiment was less than 1%.
- iii. **Correlation between the Fresnel reflection signal, temperature, and cross-linking:** Close inspection of the data [see Figure 4(b)] during the first 20 minutes after the onset of heating shows that the Fresnel signal dropped by  $\sim 12\text{--}20\%$ ; this is because the density of the resin system decreases as

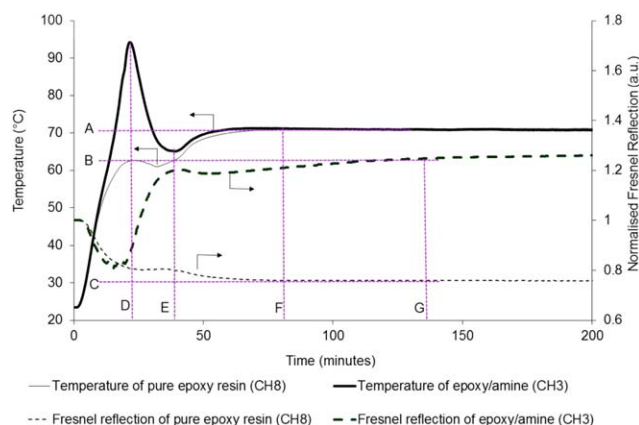


**Figure 5.** Comparison of the relative outputs from the Fresnel reflection sensors and thermocouples for the neat epoxy resin (channel 8) and the cross-linking reactions (channel 3) involving the epoxy/amine resin system. [Color figure can be viewed in the online issue, which is available at [wileyonlinelibrary.com](http://wileyonlinelibrary.com).]

it is heated because of thermal expansion.<sup>32,33</sup> In the absence of chemical reactions, degradation, or volatility of the constituent components in the resin, it can be assumed that the refractive index will decrease with increasing temperature. The refractive index is defined as the ratio of the velocity of light in a vacuum to that in the medium (resin system). With reference to Figure 4(b), the normalized refractive index decreases initially with heating because of the decrease in the density and the concomitant increase in the volume. As the temperature is increased further, at some point the cross-linking reactions proceed at an appreciable rate. In other words, as far as the refractive index of the resin system is concerned, two competing effects have to be considered: firstly, the density decreases in the initial heating period and then secondly, as evident in Figure 4(b), it increases as cross-linking reactions predominate.<sup>34–36</sup> However, as mentioned previously, the cross-linking reactions are exothermic and if isothermal conditions are not maintained, this temperature excursion will accelerate the rate of consumption of the reactive functional groups. This is generally referred to as the auto-acceleration of cross-linking reactions [37]. Therefore, it is not straightforward to decouple these various factors with regard to their respective contribution to the magnitude of the Fresnel reflection signal during the initial stages of the cross-linking reactions. This issue is discussed further when considering Figure 5.

- iv. The dip in the temperature and the effect on Fresnel signals after ~40 minutes: As the maximum temperature that was reached during the exotherm was approximately 95°C (25°C above the set temperature), the oven door was opened briefly to verify visually that the resin had not degraded. This accounts for the decrease in the recorded temperature to below the set value of 70°C; when the oven door was closed, the temperature equilibrated back to 70°C. A corresponding increase in the Fresnel reflection signal was observed when the temperature was lowered followed by an increase to an equilibrium value. After approximately

420 minutes, the Fresnel signals in the epoxy/amine vials had increased by ~17–30% when compared to their respective values prior to heating. After this period, the oven was switched off and allowed to cool; after 440 minutes (~60°C), the oven door was opened to accelerate the cooling of samples to ambient temperature.

In order to analyze the output from the sensors in detail, only the data for the Fresnel reflection signal as a function of temperature for the epoxy/amine resin system (channel 3) and the neat epoxy without the amine hardener (channel 8) are presented in Figure 5. Horizontal lines (A, B and C) have been superimposed on Figure 5 to indicate the magnitudes of the temperature and the normalized Fresnel reflection data; the vertical lines (D–G) have been superimposed to indicate the specified time during processing.

It is apparent from Figure 5 that the temperature profile for the neat epoxy resin as a function of time shows an inverse relationship with the Fresnel signal. In other words, as the temperature is increased, the Fresnel signal decreases proportionally and vice versa; thus, the time taken for an equilibrium value to be reached for the temperature and the Fresnel signal is similar. The effect of opening the oven door is once again apparent in the Fresnel reflected signal where an increase is observed as the temperature is lowered.

With reference to Figure 5, the temperatures recorded by the two thermocouples (line A) for the neat epoxy and the epoxy/amine resin system show that an equilibrium value of ~70°C was attained after approximately 60 minutes (line F). The Fresnel signal for the neat epoxy is also seen to equilibrate at 70°C after 60 minutes. However, this was not the case for the Fresnel signal for the epoxy/amine resin system where an equilibrium value was attained after approximately 140 minutes (line G). The observed differences may be attributed to the following: (a) The magnitude of the exotherm where the peak temperature recorded by the thermocouple for the amine/epoxy resin system was 94.2°C; here the rapid increase in the temperature would have accelerated the formation of the cross-link networks. As the temperature was relatively constant after approximately 60 minutes, the gradual increase in the Fresnel signal can be attributed to the gradual increase in the cross-link density, in the diffusion-controlled phase of the cross-linking reactions, until cessation after approximately 140 minutes. (b) The temperature of the oven was lowered to approximately 65°C when the oven door was opened to inspect the samples as mentioned previously.

With reference to time-line (D) for the epoxy/amine resin, it is seen that the time for the peak temperature recorded by the thermocouple does not coincide with the minimum value for the Fresnel reflection signal. As, the synchronization between the thermocouples and the Fresnel data are reliable, the following explanation is proposed: In the case of the epoxy/amine resin system, as it is heated, the refractive index decreases. However, above a certain temperature range, the cross-linking reactions commence, and the reaction rate increases as a function of temperature. Thus, initially, the heating phase dominates the decrease in the refractive index and then the cross-linking

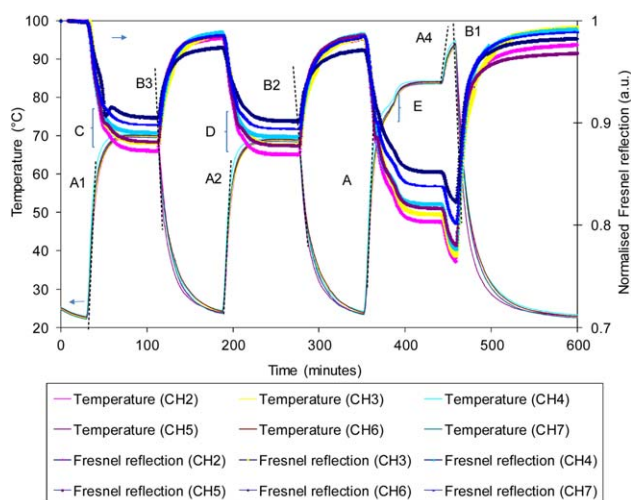


**Figure 6.** Postcure thermal cycling and the responses of the Fresnel sensors for the cured epoxy/amine resin system and the corresponding data from the thermocouples. [Color figure can be viewed in the online issue, which is available at [wileyonlinelibrary.com](http://wileyonlinelibrary.com).]

reactions dominate. In situations where a large exotherm is observed, unlike the case where isothermal conditions prevail, it will be difficult to decouple the contribution of temperature and cross-link density to the refractive index.

On inspecting the thermocouple data for the neat epoxy and the epoxy/amine resin system, it can be observed that the two samples experience the same heating rate until about 55°C; as the temperature of the oven was preset to attain 70°C, the temperature-controller reduces the rate of power input to the heaters to prevent over-shooting the set temperature. This reduction in the rate of heating within the oven is also seen in the Fresnel reflection data from the neat epoxy resin. As mentioned previously, the effect of opening the oven door is also evident in the Fresnel data for the neat resin. After the oven door was closed, the temperature within the neat epoxy sample rose steadily (period between lines E and F) until the set temperature was reached.

### Postcure Thermal Cycling

The cured resins and the neat epoxy (no amine hardener) samples were subjected to three sequential heating and cooling regimes, and the responses of the Fresnel sensors and the thermocouples were recorded. During the first two cycles, the oven was heated from ambient to 70°C and cooled back to room temperature with the oven door closed. After the third heating/cooling cycle, the samples were heated to 78°C and held for 1–2 minutes and then ramped to approximately 84°C to dwell for ~30 minutes. Subsequently, it was ramped to 94°C after which the power to the oven was switched off and allowed to cool naturally with the oven door closed.

The output data for the Fresnel sensors for the epoxy/amine resin system and the corresponding thermocouples are presented in Figure 6.

In Figure 6, consideration is given initially to the thermocouple data where linear regression lines have been superimposed on

the linear portions of the heating (A1–A4) and cooling (B1–B3) regimes; the criterion for performing the linear regression was to obtain the rates of heating and cooling. The coefficient of determination ( $R^2$ ) was 0.99. A summary of the slopes for the temperature channel 3 is presented in Table II where it can be seen that slopes A1 and A2 are similar. However, the rate for A3 is relatively higher and is probably because of the higher set temperature. The slope for A4 is lower because the set temperature of 94°C is relatively close to the preceding dwell temperature of 84°C. The same conclusion can be reached for the cooling rates (slopes B1–B3) from Table II.

As stated previously, the temperature controller adjusts the heating rate at approximately 25°C below the set isothermal temperature. This is evident on inspecting the slopes and the data from the thermocouples for the first and second temperature cycles. The heating regime for the third cycle, which accounts for the short dwell of 1–2 minutes at 78°C followed by a 30 minute dwell at 84°C, shows the modulations imposed by the temperature controller. The third heating regime was used to investigate if: (i) any additional cross-linking had taken place; and (ii) the glass transition temperature ( $T_g$ ) could be detected by the Fresnel sensors.

On inspecting the Fresnel data in Figure 6, the overall trends for channels 2–8 look similar but some anomalies are apparent. For example, (i) Figure 7(a) (expanded view of Figure 6) shows an uncharacteristic fluctuation in the data are observed for channel 6 within the region “A”. As the resin in the vial was already cross-linked, the anomaly may have been caused by some unintentional perturbation of the optical fiber connectors that were located outside the oven. Moreover, this feature in channel 6 is not observed in the two subsequent heating and cooling cycles. However, three further possible contributing reasons for the anomaly need to be considered. Firstly, considering the situation prior to cross-linking but during the first heating regime (to cross-link the resin), the coefficient of thermal expansion of the liquid epoxy/amine resin is higher than that of the optical fiber. This difference in the thermal expansion is “locked” when the resin cross-links to an infusible solid. When the assembly is cooled to room temperature, residual stresses will develop. Hence, during the cooling cycle, debonding between the optical fiber and the matrix can occur. This may not be a repeatable process because it will also depend on the magnitude of interfacial bond strength. Secondly, it is also worth noting that the resin shrinks as it cross-links and this too will contribute to the magnitude of the residual stresses. Finally, the  $T_g$  needs to be considered when the postcured resin is subjected to further heating. If the heating regime transgresses the  $T_g$  of the cross-linked polymer, properties such as the heat capacity, specific volume, and stiffness undergo a reversible change.<sup>34,38,39</sup> The unfortunate complication in the current experiment is the fact that the  $T_g$  is in the same temperature range over which the temperature controller on the oven adjusts the power input as the preset isothermal temperature is approached. (ii) Channels 3, 5, and 7 show a distinct inflection region over the period marked “A”.

Figure 7(b) shows an expanded view of the second postcure heating cycle. The anomaly observed previously for channel 6 is



**Table II.** Heating and Cooling Rates from Figure 6 for the Cured Resin (CH 3) During the Post-Cure Heating/Cooling Regimes

Slopes for specified regression lines				
Heating Rate	A1	A2	A3	A4
(°C minute <sup>-1</sup> )	3.51	3.00	3.72	0.77
Cooling Rate	B1	B2	B3	-
(°C minute <sup>-1</sup> )	-2.89	-2.23	-2.20	-

not apparent but the inflection point is present for channel 5 within zone-A.

An expanded view of the third heating and cooling cycle is presented in Figure 7(c) where three time zones of interest (A, B, and C) have been highlighted. Zones A and B show the inflection points mentioned previously. The third heating cycle involved ramping the samples from room temperature to 78°C

with a short dwell of 1–2 minutes and then a temperature ramp to 84°C with a dwell for ~30 minutes; this is clearly observable in the Fresnel and thermocouple data in zone B. An expanded section of zone-A is presented in Figure 7(d) where the inflection points are clearly visible.

With regard to the cooling curves for channels 2–7 [zone C of Figure 7(c)], the trends for the Fresnel sensors seem to reflect the temperature profile inside the oven. In other words, the inflection regions are not detected for any of the samples.

The final part of this discussion is concerned with the relative outputs from the neat epoxy sample (channel 8) and one of the cured samples that was subjected to three heating/cooling cycles (channel 3). The Fresnel sensor and thermocouple data from channels 3 and 8 is presented in Figure 8. The trends in the thermocouple data were discussed previously; therefore the current discussion is focused on the Fresnel sensor outputs for these two datasets.

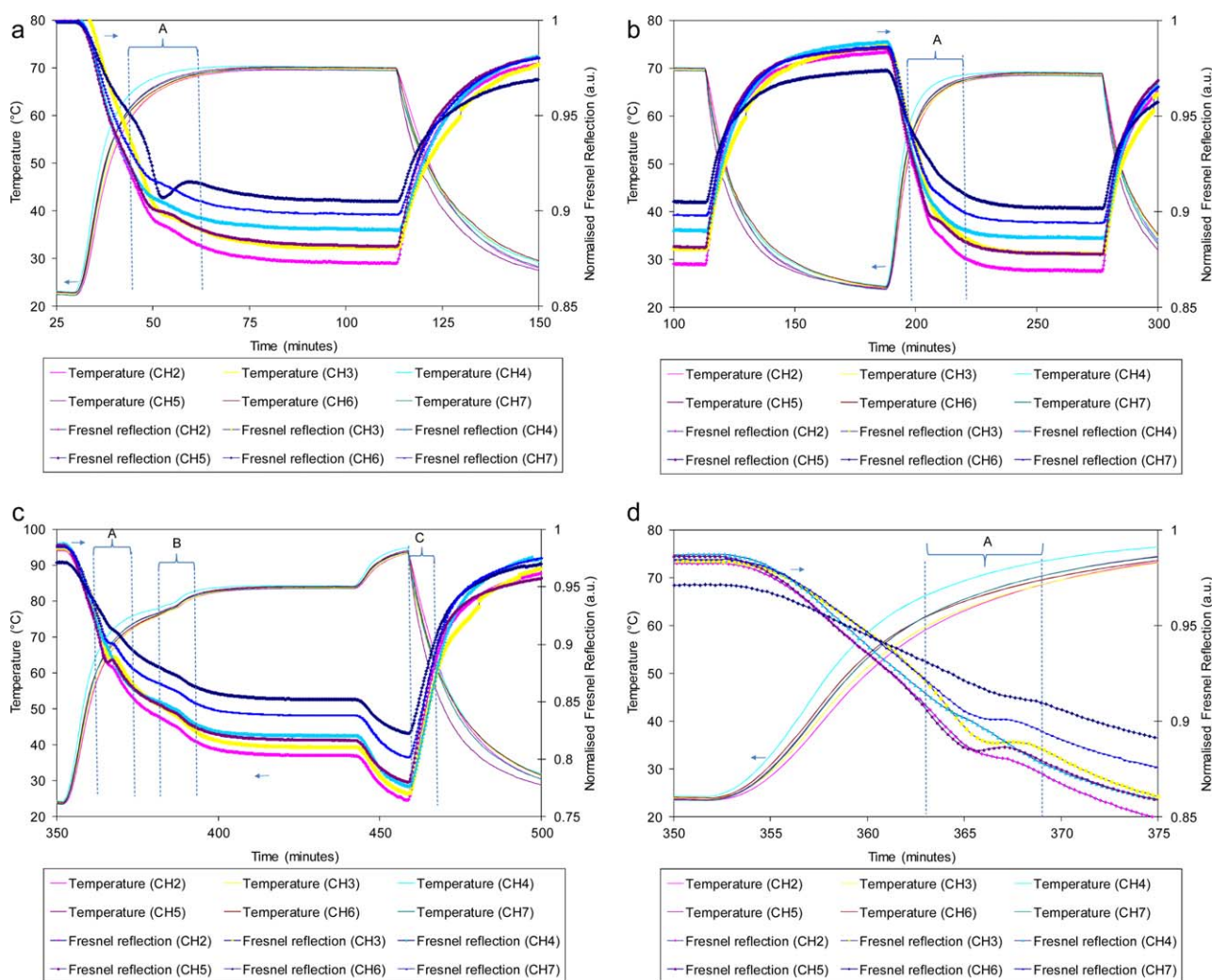


**Figure 7.** (a) An expanded view of Figure 6 showing the first postcured heating and cooling cycle. (b) An expanded view of the second heating and cooling cycle for the postcured resins where the temperature and Fresnel reflection data are presented. (c) An expanded view of Figure 6 where the third heating and cooling cycle is shown for the Fresnel sensor and thermocouple data. (d) A magnified view of Figure 6 illustrating the inflection points in the Fresnel sensor data during the third heating cycle. [Color figure can be viewed in the online issue, which is available at [wileyonlinelibrary.com](http://wileyonlinelibrary.com).]

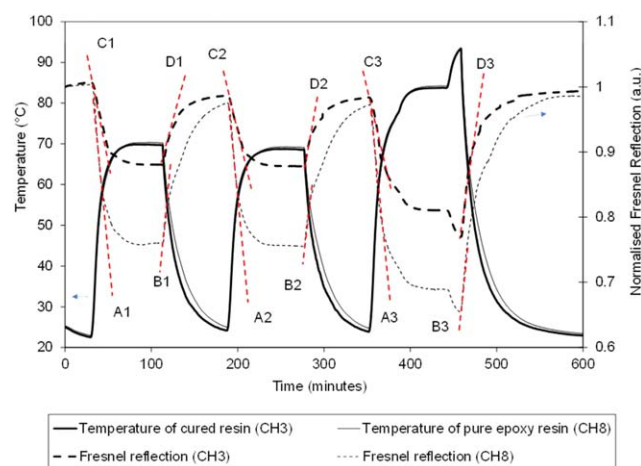


**Figure 8.** Responses of Fresnel sensors for the cured epoxy/amine resin (channel 3) and the neat epoxy resin (channel 8). The data from the corresponding thermocouples from each vial are also presented. [Color figure can be viewed in the online issue, which is available at [wileyonlinelibrary.com](http://wileyonlinelibrary.com).]

With reference to the neat epoxy Fresnel sensor data presented in Figure 8, linear regression lines (A1–A3) were calculated as described previously for the three sequential heating cycles. A summary of the slopes for these regression lines is presented in Table III; it is apparent that the slopes are similar and the deviation from linearity starts at about  $\sim 50^{\circ}\text{C}$  for the first two cycles and approximately  $55^{\circ}\text{C}$  for the third cycle. The characteristics of the Fresnel signals (B1–B3) during the cooling phase of the neat resin also show a similar dependence on temperature. In this instance, deviation from linearity is observed at approximately  $45^{\circ}\text{C}$  for the three cooling cycles; this corresponds to the time when the oven was switched off and permitted to cool.

The corresponding Fresnel sensor output for the cured epoxy/amine sample during heating (C1–C3) show a similar dependency on temperature. However, in the case of the third heating cycle (where the sample was heated from ambient to  $80^{\circ}\text{C}$ ), a distinct change in the slope is observed. This is concurrent with the trends observed for the neat epoxy sample. The trends during the cooling phase are represented by lines (D1–D3). A linear behavior is observed from  $93^{\circ}\text{C}$  to  $65^{\circ}\text{C}$ ; the change in slope for the cured resin after  $65^{\circ}\text{C}$  is mirrored in that observed for the temperature profile and the neat epoxy resin.

A further analysis of Figure 8 is presented in Figures 9(a and b) representing the time derivatives of normalized Fresnel reflection (NFR) and the corresponding temperature for channels 8

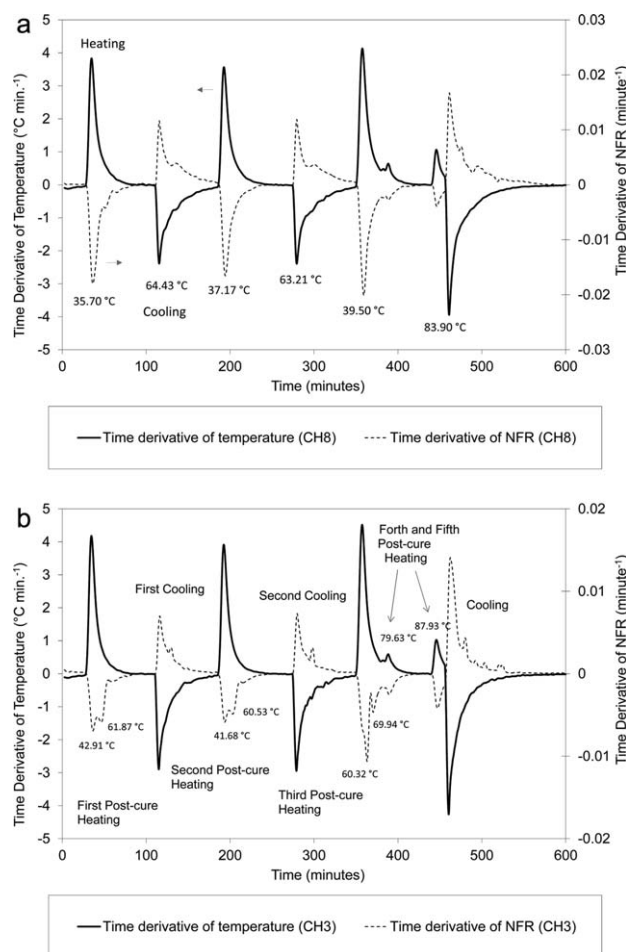


**Figure 9.** (a) Time derivatives from Figure 8 for the NFR and temperature data for channel 8 (neat resin). (b) Time derivatives from Figure 8 for the NFR and temperature data for channel 3 (cross-linked resin).

(neat resin) and 3 (epoxy/amine cure) respectively. It is readily apparent from Figure 9(a), that the plots of the derivatives of NFR and temperature show mirror-image-like trends for the neat epoxy. In Figure 9(a), the perturbation observed in the Fresnel signal may have been because of mechanically induced perturbations caused by opening/closing of the door of the oven. Figure 9(b) shows the time-derivative data for channel 3 (epoxy/amine resin system). Peak-splitting is seen in the time-derivative of the NFR data as the cross-linked resin is heated to the set temperature. As this feature was not observed in for the neat epoxy resin, it is concluded that the peak-splitting may be a manifestation of  $T_g$  the resin system. The  $T_g$  obtained via a differential scanning calorimeter is generally defined as the mid-

**Table III.** Slopes of the Fresnel Signals from Channels 3 and 8 during the Post-Cure Thermal Cycles as Shown in Figure 8

Slopes for specified regression lines						
Fresnel signal (Neat resin - CH8)	A1	A2	A3	B1	B2	B3
	-0.0169	-0.0140	-0.0184	0.0046	0.0085	0.0130
Fresnel signal (Cured resin - CH3)	C1	C2	C3	D1	D2	D3
	-0.0064	-0.0051	-0.0055	0.0030	0.0055	0.0123

point of the inflection in the thermogram. With the current resin system, the  $T_g$  was measured to be in the region of 75°C. It is worth noting that the glass transition is a second-order transition ( $T_g$ ) and its value will depend on the technique (dynamic mechanical thermal analysis, differential thermal analysis, torsional braid, etc) that is used to obtain it.<sup>32–39</sup>

## CONCLUSIONS

In this study, six independent Fresnel sensors were immersed in vials containing an epoxy/amine resin system and cross-linked in an oven. A thermocouple was also co-located in the vials to monitor the temperature. Two additional sensors were also used: one was immersed in a neat epoxy sample (no hardener) which was placed alongside the six epoxy/amine specimens, and the other was immersed in an index-matched gel and placed outside the oven. After cross-linking, the cured specimens and the vial containing the neat epoxy resin were subjected to three successive heating and cooling regimes.

The following conclusions were reached: (i) multiple Fresnel sensors can be used in tandem with an optical switching unit to track the cross-linking process at specified locations; (ii) the Fresnel sensor is sensitive to temperature; (iii) under isothermal conditions, it is possible to infer the cross-linking rate and when an equilibrium value is attained. However, it is necessary to bear in mind that the exotherm can complicate the interpretation of the Fresnel signal if the temperature is not monitored independently; (iv) the Fresnel sensors can be used after curing to study the effects of heating and cooling; (v) the derivative of the NFR for the epoxy/amine resin system showed peak-splitting during the heating cycle, this may be indicative of the glass transition temperature.

## ACKNOWLEDGMENTS

The authors wish to acknowledge financial support from the EPSRC (TS/G000387/1) and the Technology Strategy Board, Projects AB134K and BD072K. The support given by the industrial partners (Pultrux, PPG, CTM, Bruker Optics, Mould Life, Luxfer Gas Cylinders, Halyard, and Huntsman Polyurethanes) is duly acknowledged. GF and VRM acknowledge the financial support provided by the Royal Society. VRM acknowledges the assistance given by Drs R.S. Mahendran, M.S. Irfan, and D. Harris for specified aspects of the experimental work. The authors wish to acknowledge the technical assistance provided by Professor Brian Ralph, Mark Paget, and Frank Biddlestone.

## REFERENCES

1. Fernando, G. F.; Degamber, B. *Int. Mater. Rev.* **2006**, *51*, 65.
2. Liu, T.; Brooks, D.; Martin, A.; Badcock, R. A.; Ralph, B.; Fernando, G. F. *Smart Mater. Struct.* **1997**, *6*, 464.
3. Machavaram, V. R.; Badcock, R. A.; Fernando, G. F. *Sens. Actuators A Phys.* **2007**, *138*, 248.
4. Doyle, C.; Martin, A.; Liu, T.; Hayes, S.; Crosby, P. A.; Brooks, D.; Badcock, R. A.; Fernando, G. F. *Smart Mater. Struct.* **1998**, *7*, 145.
5. Degamber, B.; Tetlow, J.; Fernando, G. F. *J. Appl. Polym. Sci.* **2004**, *94*, 83.
6. Martin, A.; Badcock, R. A.; Nightingale, C.; Fernando, G. F. *IEEE Photonics Technol. Lett.* **1997**, *9*, 982.
7. Sorensen, L.; Gmur, T.; Botsis, J. *Composite A* **2006**, *37*, 270.
8. Tanaka, N.; Okabe, Y.; Takeda, N. *Smart Mater. Struct.* **2003**, *12*, 940.
9. Liu, T.; Wu, M.; Fernando, G. F.; Rao, Y. J.; Jackson, D. A.; Zhang, L.; Bennion, I. *Smart Mater. Struct.* **1998**, *7*, 550.
10. James, S. W.; Ralph, P. T. *Meas. Sci. Technol.* **2003**, *14*, 49.
11. Mahendran, R. S.; Machavaram, V. R.; Wang, L.; Burns, J. M.; Harris, D.; Kukureka, S. N.; Fernando, G. F. *SPIE* **2009**, 7293, C1.
12. Fernando, G. F.; Liu, T.; Crosby, P. A.; Doyle, C.; Martin, A.; Brooks, D.; Ralph, B.; Badcock, R. A. *Meas. Sci. Technol.* **1997**, *8*, 1065.
13. Wang, L.; Pandita, S.; Machavaram, V. R.; Malik, S.; Harris, D.; Fernando, G. F. *Compos. Sci. Technol.* **2009**, *69*, 2069.
14. Born, M.; Wolf, E. In *Principles of Optics*, 7th ed.; Cambridge University Press: Cambridge, **1999**.
15. Crosby, P. A.; Powell, G. R.; Fernando, G. F.; France, C. M.; Waters, D. N.; Spooncer, R. C. *Sensors Ser.* **1995**, Institute of Physics, Dublin, 10–13 September.
16. Cusano, A.; Cutolo, A.; Giordano, M.; Nicolais, L. *IEEE Sens. J.* **2003**, *3*, 781.
17. Vacher, S.; Molimard, J.; Gagnaire, H.; Vautrin, A. *Polym. Polym. Compos.* **2004**, *12*, 269.
18. Aduriz, X. A.; Lupi, C.; Boyard, N.; Bailleul, J. L.; Leduc, D.; Sobotka, V.; Lefevre, N.; Chapeleau, X.; Boisrobert, C.; Delaunay, D. *Compos. Sci. Technol.* **2007**, *67*, 3196.
19. Crosby, P. A.; Powell, G. R.; Fernando, G. F.; France, C. M.; Spooncer, R. C.; Waters, D. N. *Smart Mater. Struct.* **2006**, *5*, 415.
20. Liu, Y. M.; Ganesh, C.; Steele, J. P. H.; Jones, J. E. *J. Compos. Mater.* **1996**, *31*, 87.
21. Huang, X. G.; Wu, Y. T.; Yang, H.; Xiong, Y. K. *J. Lightwave Technol.* **2009**, *27*, 2583.
22. Chen, J. H.; Huang, X. G.; He, W. X.; Tao, J. *Opt. Laser Technol.* **2011**, *43*, 1424.
23. Chen, J. H.; Huang, X. G. *Opt. Commun.* **2010**, *283*, 1674.
24. Cusano, A.; Breglio, G.; Giordano, M.; Calabro, A.; Cutolo, A.; Nicolais, L. *Sens. Actuators A Phys.* **2000**, *84*, 270.
25. Chang, K. A.; Lim, H. J.; Su, C. B. *Meas. Sci. Technol.* **2002**, *13*, 1962.
26. Kim, C. B.; Su, C. B. *Meas. Sci. Technol.* **2004**, *15*, 1683.
27. Buggy, S. J.; Chehura, E.; James, S. W.; Tatam, R. P. *J. Opt.* **2007**, *9*, S60.
28. Giordano, M.; Laudati, A.; Russo, M.; Nasser, J.; Persiano, G. V.; Cusano, A. *Thin Solid Films* **2004**, *450*, 191.
29. Mahendran, R. S.; Wang, L.; Machavaram, V. R.; Pandita, S. D.; Chen, R.; Kukureka, S. N.; Fernando, G. F. *Opt. Laser Eng.* **2009**, *47*, 1069.

30. Dimopoulos, A.; Buggy, S. J.; Skordos, A. A.; James, S. W.; Tatam, R. P.; Patridge, I. K. *J. Appl. Polym. Sci.* **2009**, *113*, 730.
31. Wang, P.; Molimard, J.; Drapier, S.; Vautrin, A.; Minni, J. C. *J. Compos. Mater.* **2011**, *46*, 691.
32. Holst, M.; Schanzlin, K.; Wenzel, M.; Xu, J.; Lellinger, D.; Alig, I. *J. Polym. Sci. Part B Polym. Phys.* **2005**, *43*, 2314.
33. Priyadarshi, A.; Shimi, L.; Wong, E. H.; Rajoo, R.; Mhaisalkar, S. G.; Kripesh, V. *J. Electron. Mater.* **2005**, *34*, 1378.
34. Chang, T. D.; Carr, S. H.; Brittain, J. O. *Polym. Eng. Sci.* **1982**, *22*, 1213.
35. Degamber, B.; Winter, D.; Tetlow, J. Fernando, G. F. *Meas. Sci. Technol.* **2004**, *15*, L5.
36. Muller, U.; Philip, M.; Gervais, P. -C.; Possart, W.; Wehlack, C.; Kieffer, J.; Sanctuary, R.; Kruger, J. K. *New J. Phys.* **2010**, *12*, 083036, 1.
37. Crosby, P. A.; Fernando, G. F. The Application of Optical Fibre Sensors in Advanced Fibre Reinforced Composites. – In Cure Monitoring, Optical Fibre Sensor Technology; Grat-tan, K. T. V.; Meggitt, B. T., Eds.; Kluwer Academic Publishers; London, **1999**; Vol *III*, Chapter 3. ISBN 0412825708.
38. Muller, U.; Philipp, M.; Thomassey, M.; Sanctuary, R.; Kruger, J. K. *Thermochem. Acta*, **2013**, *555*, 17.
39. Yu, H.; Mhaisalkar, S. G.; Wong, E. H. *Macromol. Rapid Commun.* **2005**, *26*, 1483.